Wood Science and Technology Vol. 4 (1970) p. 50—69

Unsteady-State Gas Permeability of Wood

By Anco L. Prak

School of Forest Resources, Department of Wood and Paper Science, Robertson Laboratory of North Carolina State University, Raleigh, N.C.

Abstract

Steady-state permeability experiments yield a single value for permeability in each of the three structural directions of wood. A high value indicates that passage through the wood is easy, but it does not necessarily mean that all voids are filled readily with a fluid.

This research aimed at developing an experimental method that would give a better insight in this "dual" nature of wood permeability.

Cylindrical wood specimens, 50 cm × 7.5 cm diameter were evacuated and a known quantity of gas was admitted to the system. A comparison of the pressure/time curve with theoretically derived results gave values for the transverse or longitudinal gas permeability.

The most important results are: 1. Several species show a definitely "dual" permeability in the transverse direction; 2. the longitudinal/transverse permeability ratio for large specimens is considerably lower than steady-state results on small specimens indicate.

Introduction

The main purpose of this research was to gain a better understanding of the porosity and interstructural communication of sizable specimens of wood under non-steady state penetration conditions.

In the case of gas or vapor permeability most of the previous experiments have been made under steady-state conditions. One advantage of the steady-state approach is that one may select relatively small and therefore reasonably uniform specimens and obtain accurate data in a relatively short period of time. There is no concern about some of the gas being absorbed, because the experiment can be carried out after internal surface absorption has proceeded to an equilibrium level. A small specimen requires only a modest pressure difference between the two faces, and the gas density may be assumed constant to a very good approximation. Steady-state flow data can be obtained to a high degree of accuracy by selecting a sufficiently long time period over which to measure the flow. The mathematics of theoretical steady-state flow rates is very simple and straightforward.

In spite of all the advantages involved in the research of steady-state permeability, there are some very good arguments that unsteady-state research is needed also. Practical applications of permeability are almost always in the unsteady-state category. Drying, evacuation and chemical treatment are examples of such applications. If wood were a material of uniform permeability, the results of steady-state experiments would be applicable to the unsteady-state situation, and predic-

Paper No. 2793 of the Journal Series of the North Carolina Agricultural Experiment Station, Raleigh, N. C.; a condensation of part of Ph. D. thesis from the Department of Wood and Paper Science of North Carolina State University 1967 under the direction of Alfred J. Stamm, Robertson, Professor of Wood and Paper Science.

tion of unsteady-state results would be a simple matter. However, steady-state permeability is a function of the most effective among the parallel alternate passages available. Some portion of the specimen may even be almost inaccessible, while the whole specimen appears highly permeable. A practical example of this is the longitudinal liquid permeability of red oak which is very high when measured by steady-state methods, while treatments of this species with liquids require a long time. This indicates that the steady-state longitudinal permeability is not directly applicable to an unsteady-state situation. Under unsteady state conditions, the relatively inaccessible voids are filled eventually.

The time lag between the filling of the easily accessible voids and the less accessible ones may be substantial. One might say that the unsteady-state longitudinal permeability is lower than its steady-state counterpart. For the transverse[1] permeability the opposite holds true. (See under "Transverse and Longitudinal Permeability of Yellow Poplar"). In fact, it would be appropriate to talk about a pore-permeability and a fiber-permeability of red oak as two different properties. A further discussion of a dual permeability concept follows later.

The practical significance of liquid permeability is obvious. However, gas phase treatments appear to have a definite potential and unsteady state experimentation is much easier in the gas phase.

The purpose of this study was to develop a method for measuring unsteady-state gas permeability and to investigate the permeability behavior of some species to helium. A series of experiments with pentane will be described in a later publication.

BAILEY [1913], STAMM [1929], BUCKMAN et al. [1935], PFALZNER [1950], RESCH and ECKLUND [1964], SEBASTIAN et al. [1965] and COMSTOCK [1965, 1967] among others have reported on steady-state permeability research. RESCH [1967] studied the unsteady-state flow of air, nitrogen and butane vapor through Douglas-fir. He used 8 inch diameter bolts, which were end-coated. He evacuated these specimens after they had been filled with nitrogen and butane, and his data apply to the removal of gaseous substances. He sealed a hollow metal probe inside the specimen and measured the pressure at the center in one bolt and at half the radius in another. He found reasonably good agreement between calculated pressure drops and those actually observed.

Experimental Method

This author elected to study the entry of gas into wood. The equipment consisted of two stainless steel bombs, 1.4 and 3.0 liters in size, four valves, a Dynisco PT 69-25 pressure transducer, a McLeod low pressure gauge, a buret and connecting stainless steel and rubber tubing, as shown in Fig. 1. Not shown in this figure are a Welch Duo Seal vacuum pump to evacuate the system and also used as reference pressure for the transducer, a Kepco ABC-10-0.75 M constant voltage supply for the excitation of the transducer and a Minneapolis-Honeywell Rubicon 2732 potentiometer to read the output of the transducer. A commercial helium

[1] The experimental procedure followed in this study does not allow separation of radial and tangential permeability. Whenever these two are confounded, the term "transverse" is used.

cylinder, a reduction valve, a drying bottle and an auxiliary vacuum pump, also not shown, completed the installation.

Cylinder 1 was entirely submerged in a constant temperature bath; cylinder 2 was submerged about 60 percent in the constant temperature bath. The part above the bath was surrounded by an electric heating mantle, and the voltage was adjusted to bring the temperature of the top part of cylinder 2 to the level of the

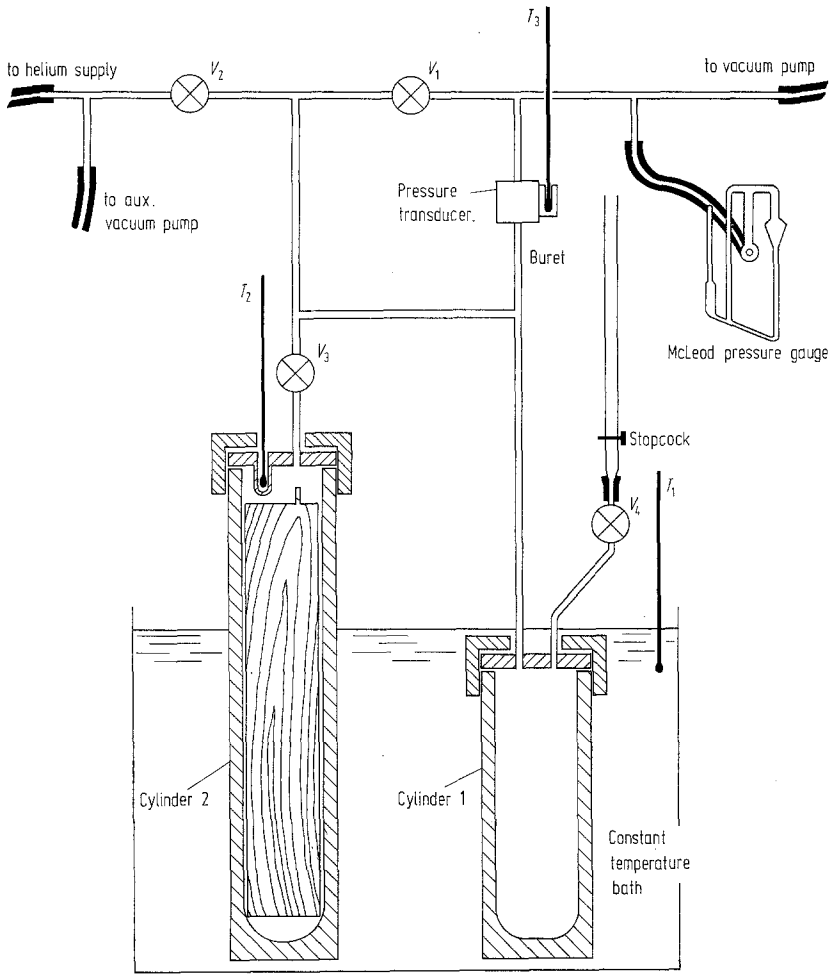

Fig. 1. Equipment for measuring unsteady-state gas permeability of wood.

bath. The tubing between valves V_2, V_1, and V_4, the pressure transducer and both cylinders, was surrounded with electrical heating wire (to avoid cold spots where pentane might condense). The temperature of these appendages was measured at the pressure transducer itself, and was kept within about 5° C of the bath temperature.

Cylindrical wood specimens, 50 cm long and 7.5 cm in diameter, were introduced in cylinder 2. The specimens, which had been oven dried previously, were

then evacuated by closing valves V_2 and V_4 and opening valves V_1 and V_3. The evacuation was continued until the pressure at the McLeod gauge read 0.035 Torr or less. The pressure surrounding the specimen then was in the order of 0.050 to 0.075 Torr. This level of vacuum was reached usually in just over 24 hours. When the evacuation was complete (in the above sense), valves V_3 and V_1 were closed. Helium gas was admitted via a drying bottle through valve V_2. An auxiliary vacuum pump was used to remove any traces of air from the helium supply system prior to its use. Helium was admitted in excess amounts followed by "bleeding" down to the required starting pressure. After helium was introduced, it was allowed to reach the temperature of the system, before any measurements were made.

The actual permeability runs were started by opening valve V_3. This allows the gas to expand from cylinder 1 into cylinder 2. The data collected are pressure and time determinations. Temperatures were read in three locations (Fig. 1) to allow for the necessary correction factors. The transducer output turned out to be temperature dependent and it was therefore calibrated at several temperature levels.

The voltage reading from the pressure transducer were converted to pressure. The pressures were converted to fraction filled and reported as such. For the purpose of this discussion, fraction filled, F_n, is defined as:

$$F_n = \frac{\text{moles of penetrant in specimen}}{\text{moles of penetrant in specimen at "gas phase equilibrium"}} \tag{1}$$

where gas phase equilibrium is defined as the condition where a uniform pressure exists throughout the specimen and the entire system, and no penetrant has been absorbed or has condensed. For helium gas, absorption may be assumed zero, and condensation is most certainly zero at the temperatures employed. Thus, the gas phase equilibrium condition for helium is simply the equilibrium obtained at the end of the experiment.

Selection and Preparation of Specimens

The main part of this research was carried out on specimens of the maximum dimension which fitted into cylinder 2 (Fig. 1). This dimension was approximately 50 cm long by 7.5 cm diameter, or 2209 cm^3. In order to be able to compare the experimental results with theoretical calculations, it was desirable to use a species which was uniform in texture.

Specimens of low permeability were most satisfactory as a great deal of pressure/time data could be collected before equilibrium was reached.

The choice of specimens was limited also by supply. A list of the specimens used in the study is given in Table 1 (see p. 54).

Of these, yellow poplar heartwood proved almost ideally suited to the work. The difference found between specimens which came out of the same logs made it clear that closely matched specimens cannot be obtained. It was, therefore, decided to use the same specimen over and over, oven-drying between runs. The bulk of the data collected was on two yellow poplar heartwood specimens, numbered II and V.

For most of the work the specimens were endcoated with epoxy resin. All experimental results apply to transverse flow into endcoated specimens, except where other conditions are specifically stated.

The specimens, when not obtained in kiln-dry form, were air-dried for two months or more and then brought indoors for a similar period. They were oven-dried from two to eight days at 105° C prior to each experimental run.

Table 1. *List of Cylindrical Specimens Used in the Study*

Species	Number of specimes
Hard Maple (*Acer spec.*) heartwood	3
Tupelo gum (*Nyssa aquatica*) sapwood	1
American beech (*Fagus grandifolia*) heartwood	1
Yellow poplar (*Liriodendron tulipifera*) heartwood	3
Yellow poplar (*Liriodendron tulipifera*) sapwood	2
Soft maple (*Acer rubrum*) heartwood	2
Douglas-fir (*Pseudotsuga taxifolia*) heartwood	1
White oak (*Quercus spec.*) heartwood	2

Theoretical Calculations of Darcy's Flow of an Ideal Gas Into an Evacuated Wood Specimen

The volumetric rate of flow q is given by

$$q = \frac{KA}{\eta} \frac{\mathrm{d}p}{\mathrm{d}x} \tag{2}$$

where A is the cross-sectional area; $\mathrm{d}p/\mathrm{d}x$ is the pressure gradient; η is the viscosity of the fluid and K the specific permeability. This equation is a form of Darcy's law and also the defining equation for the specific permeability.

By making use of Darcy's law, the ideal gas law and the geometric relations applying to a cylinder, it can be shown that

$$\frac{\partial p}{\partial t} = \frac{K}{2\phi\eta} \frac{1}{x} \frac{\partial}{\partial x} \left[x \frac{\partial (p^2)}{\partial x} \right] \tag{3}$$

where p is the pressure; t is the time elapsed form the start (when $p = 0$); ϕ is the porosity and x is the radius at which p is determined. This calculation holds for a cylindrical specimen with endcoating such that all of the gas flow is transverse.

The parabolic partial differential Eq. (3) can also be given in the integrated form:

$$p\ (x, t) = \frac{K}{2\phi\eta x} \frac{\partial}{\partial x} \left[x \int_0^t \frac{\partial (p^2)}{\partial x}\, d\tau \right]. \tag{4}$$

Eqs. (3) and (4) are subject to the following boundary conditions:

$$\begin{aligned} p(x, 0) &= \vartheta(x - r)\,, \\ p(x, t) &= P_{\mathrm{ex}} \text{ for } x \geq r \\ p(x, t) &\to P_{\mathrm{ex}} \text{ for } t \to \infty. \end{aligned}$$

No rigorous analytical solution for these equations has been derived. However, when one introduces certain simplifying assumptions, it is possible to derive numerical solutions and find the pressure gradient for different levels of t. These simplifying assumptions primarily involve dividing the specimen into concentric zones with constant pressures. The flow from each zone to the next can be calculated and the pressure of the zones is instantaneously adjusted at the end of each flow period. The gradients in Fig. 2 are based on 10 concentric zones and over 1,000,000 flow periods of equal duration.

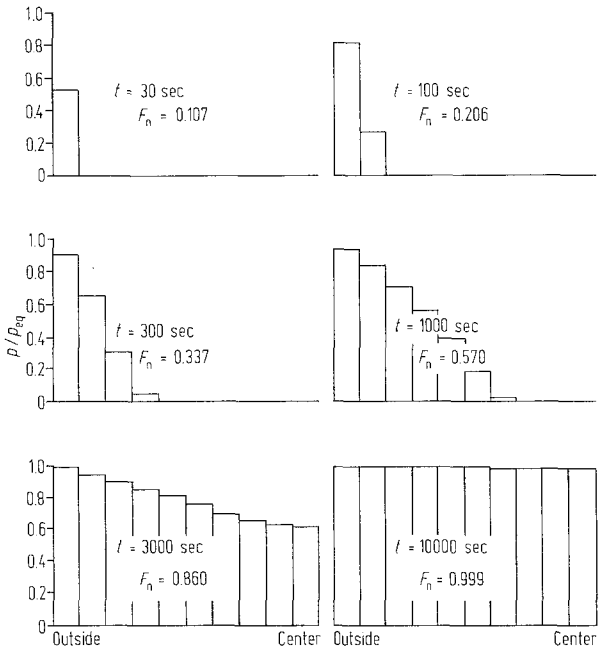

Fig. 2. Pressure gradients from numerical solutions; external pressure held constant. Pressures expressed as a fraction of equilibrium pressure Helium; $T = 40$ °C; $p_{eq} = 330$ Torr; $K = 0.94 \cdot 10^{-12}$ cm². F_n = Fraction filled.

The experimental arrangement is such that the flow is calculated from the drop in external pressure. It is therefore impossible to conduct the experiment holding the external pressure constant. Instead the experiment was conducted in a closed system. The numerical solution involves merely the introduction of one additional zone which is the free gas surrounding the specimen and in cylinder 2 (Fig. 1). The gradients for the constant volume experiment are shown in Fig. 3 (see p. 56).

As explained above, there are no provisions in the experimental setup to measure the pressure at any place except the surroundings. Thus the pressure gradients of Fig. 3 cannot be verified experimentally. However, the fraction filled as a function of time can be calculated from the numerical solutions and from experimental data. Fig. 4 (see p. 56) shows such a comparison for yellow poplar heartwood and Fig. 5 (see p. 57) for Douglas-fir.

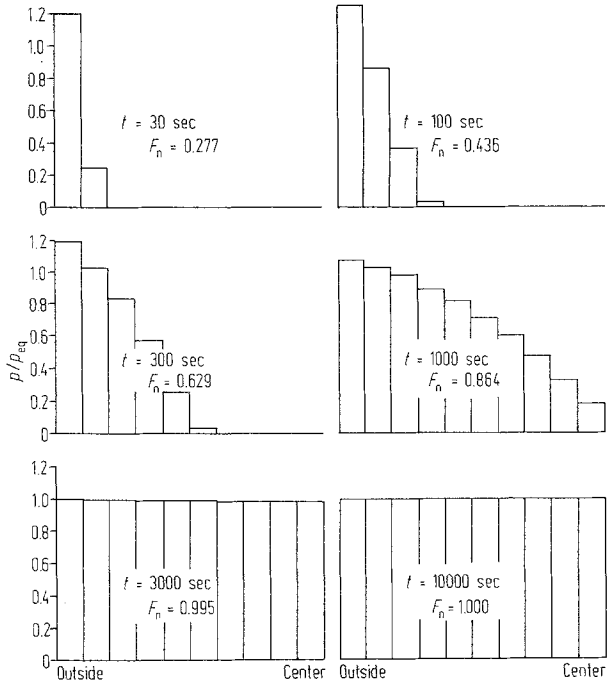

Fig. 3. Pressure gradients from numerical solutions; finite surroundings. Pressures expressed as a fraction of equilibrium pressure; Helium; T = 40 °C; p_{eq} = 330 Torr; $K = 0.94 \cdot 10^{-12}$ cm². F_n = Fraction filled.

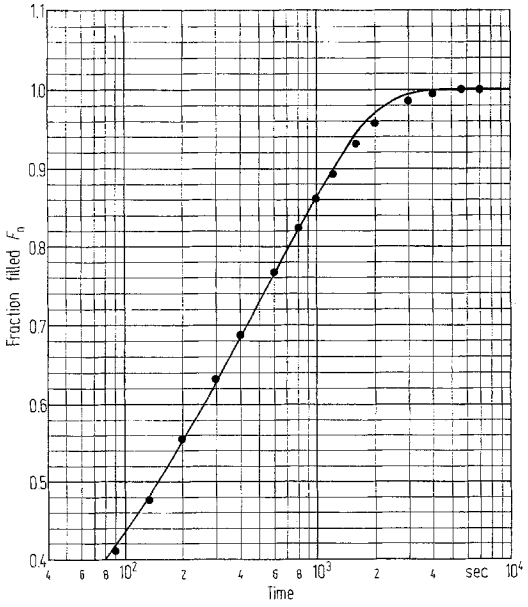

Fig. 4. Comparison of experimental data for yellow poplar and numerical solution for simple model. Yellow poplar specimen II heartwood; run 12; Helium; T = 40 °C; p_{eq} = 329 Torr; $K = 0.94 \cdot 10^{-12}$ cm². Curve is numerical solution for same conditions.

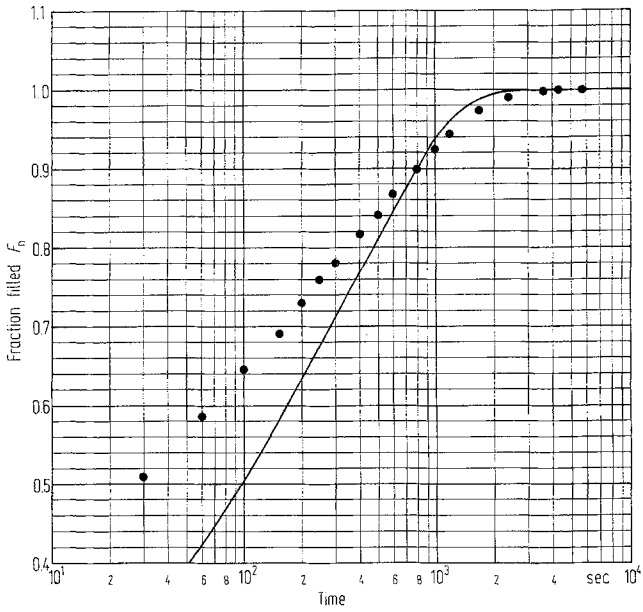

Fig. 5. Comparison of experimental data for Douglas-fir and numerical solution for simple model. Douglas-fir specimen I; run 4; Helium; $T = 40$ °C; $p_{eq} = 340$ Torr; $K = 1.43 \cdot 10^{-12}$ cm². Curve is numerical solution for same conditions.

The disagreement between the experimental results and the theory suggests that the validity of the simple model, consisting of 10 concentric zones with equal permeability, although good for yellow poplar, is poor for Douglas-fir. In view of the many different categories of cavities and passages, it is indeed surprising that a model with uniform permeability gives such good results as shown in Fig. 4.

Several models may be constructed allowing for two levels of permeability. Figs. 6 and 7 give two such models. Model A has the same configuration as the simple model with the inclusion of a large number of small isolated zones of lower permeability. For the purpose of the calculations shown later, the geometry of

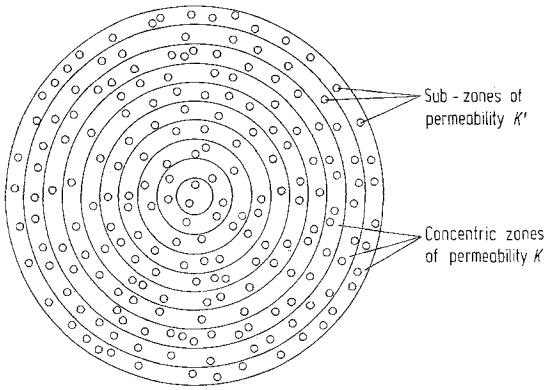

Fig. 6. Model A showing sub-zones of lower permeability.

these zones was arbitrarily chosen as a set of cylinders, parallel to the specimen axis and 0.1 cm in diameter. For such a model there are three parameters of interest, namely, the permeability K of the main portion of the specimen, the permeability ratio K'/K giving the relative permeability of the small isolated zones and volume fraction α made up by the isolated zones. (The size of these isolated zones is immaterial in the sense that for every size a ratio K'/K can be found giving the same result.)

Fig. 7 gives a model where the greater part of the volume has the lower permeability. Compared to the low permeability of the sub-zones, the permeability of

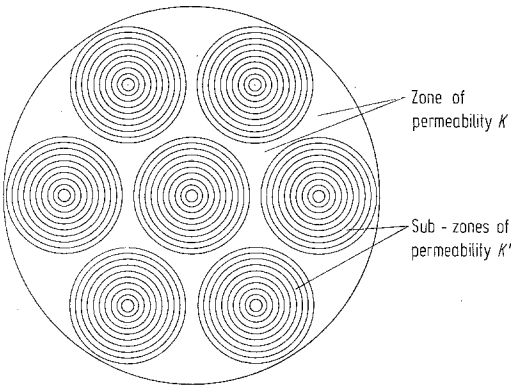

Fig. 7. Model B showing sub-zones of lower permeability.

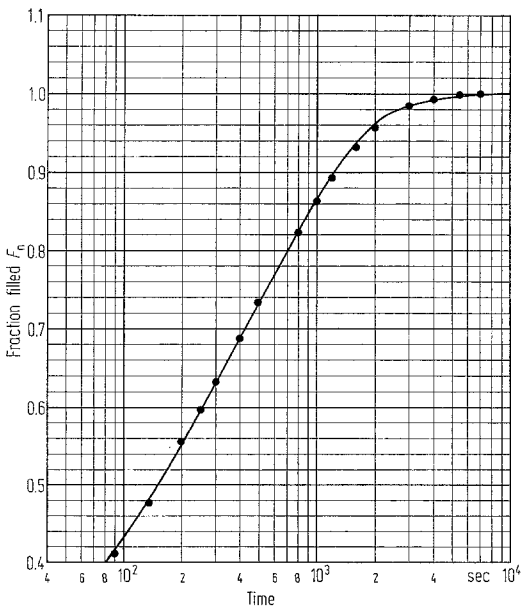

Fig. 8. Comparison of experimental data for yellow poplar and numerical solution for model A. Yellow poplar specimen II heartwood; run 12; Helium; $T = 40$ °C; $p_{eq} = 329$ Torr; $K = 1.09 \cdot 10^{-12}$ cm^2; $\alpha = 0.06$; $K'/K = 0.0003$. Curve is numerical solution for same conditions.

the surrounding tissue has been assumed ∞. Each of the sub-zones is a reduced size copy of the simple model.

When the appropriate levels for these constants are used, it is possible to match the experimental results for yellow poplar to a very high degree. Fig. 8 shows the same experimental data as shown in Fig. 4, superimposed on a curve calculated for model A with $\alpha = 0.06$ and $K'/K = 0.0003$. Because the required level of α is 0.06, the conclusion may be drawn that yellow poplar heartwood has a permeability that is constant for the remaining fraction 0.94. (This statement is obviously only true in a macroscopic sense. The different diameters of pores and lumen clearly indicate that microscopically there are substantially different levels of permeability.)

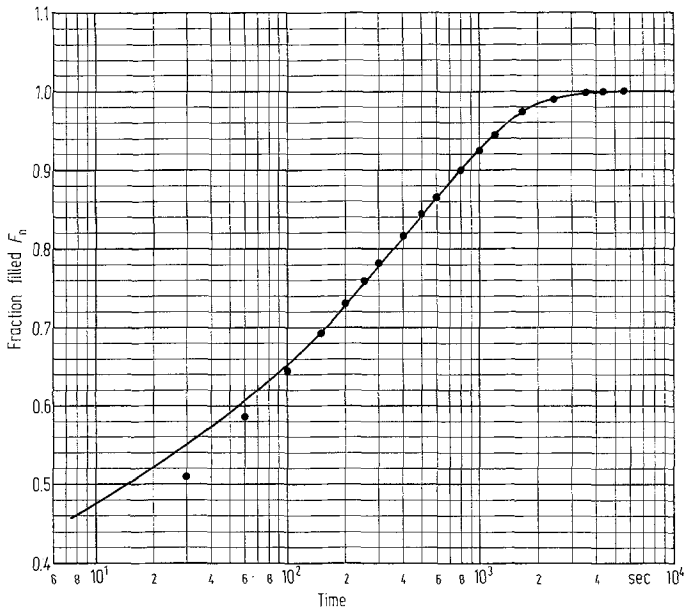

Fig. 9. Comparison of experimental data for Douglas-fir and numerical solution for model B. Douglas-fir specimen I; run 4; Helium; $T = 40$ °C; $p_{eq} = 340$ Torr; $K' = 0.148 \cdot 10^{-12}$ cm²; $\alpha = 0.63$; $K = \infty$. Curve is numerical solution for model B as shown in Fig. 7.

Fig. 9 shows how model B will give results that closely correspond to the experimental data for a Douglas-fir specimen. It should be noted that the only deviation between the experimental results and the calculated curve occurs in the region below 120 seconds. This deviation is to be expected because the assumption of an infinite permeability for the tissue surrounding the low permeability zones causes the curve to originate from a point $t = 0$, $F_n = 0.37$. The infinity assumption was needed in order to have a calculable model. If a high but finite permeability is chosen, the early part of the curve will approach the experimental data.

Another observation must be made about model B. The easy penetration of some central portion of the specimen corresponds to the experimental situation

that applies to specimens with major drying defects. Douglas-fir is one species of which no perfectly dried specimen was obtained. The specimen used for Figs. 5 and 9 had some cracks which did not appear to go down very deep at the time of the experiment.

In conclusion it can be said that with the assumption of more than one level of permeability the theory will explain the various shapes of curves, as shown in Figs. 8 and 9. However, when the work is restricted to a species like yellow poplar, the simple model is quite satisfactory.

In the following presentation of experimental results, all specimens are assumed to have a single level of permeability. The main reason for not making use of the more elaborate models A and B in interpreting the data is that no conclusions may be drawn about the relative level of permeability. The levels found to result in the curves of Figs. 8 and 9 are completely dependent on the arbitrary assumptions for the geometry of the zones. The only quantity that appears to have physical significance is the volume fraction α.

Experimental Results

The experimental results, other than the foregoing indication that Darcy's flow can predict to a good approximation the flow of gases through wood, are manifold. The experimental data are given under the following headings:

1. Permeability of several species.
2. Variation of permeability between Douglas-fir specimens.
3. Transverse and longitudinal permeability of yellow poplar.
4. Some evidence in support of the slip flow theory.
5. Specific gravity of wood substance.

Permeability of Several Species

Inasmuch as the availability of specimens was limited, the data collected do not constitute a catalogue of permeabilities of many species. Several species were used in the helium experiments before yellow poplar was selected as the most suitable for the work with different size gas molecules. The data obtained for these different species are shown in Figs. 10, 11 and 12. Figs. 10 and 11 give fraction filled as a function of time for 10 specimens of seven species, none of which were endcoated. While the dimensions of commercial timber will rarely be identical to that of the specimens (50 cm $\times$ 7.5 cm diameter), the data nevertheless give some measure of what might be termed "industrial" gas permeability.

The theory has been developed for a system allowing only transverse flow. This means that a quantitative evaluation of permeability must be restricted here to the experimental runs with endcoated specimens. The results for five runs of four species are shown in Fig. 12. Using an arbitrary level of fraction filled $= 0.9$ as a measure, the permeability of the endcoated specimens has been calculated. The results are shown in Table 2.

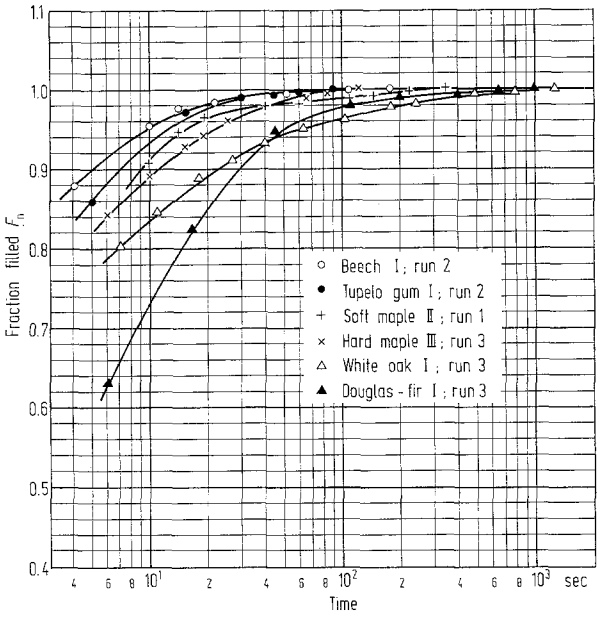

Fig. 10. Total gas permeability for six species. Specimen without endcoating; Helium; T = 40 °C; p_{eq} = 331 ... 372 Torr.

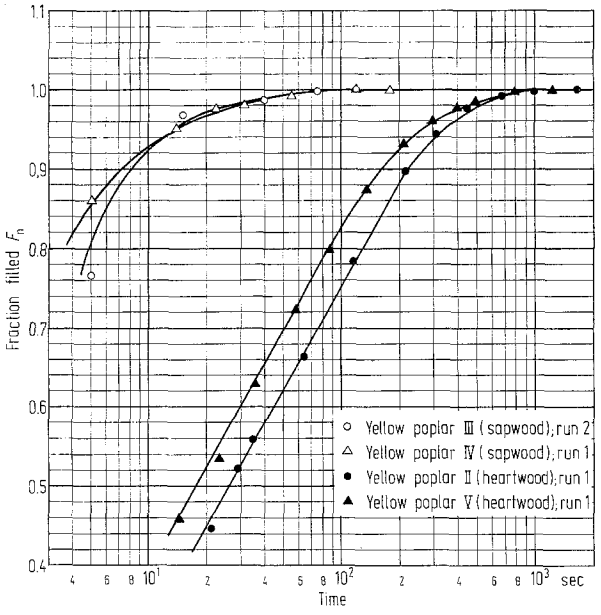

Fig. 11. Total gas permeability; yellow poplar heartwood and sapwood. Specimens without endcoating; Helium; T = 37 ... 40 °C; p_{eq} = 332 ... 336 Torr.

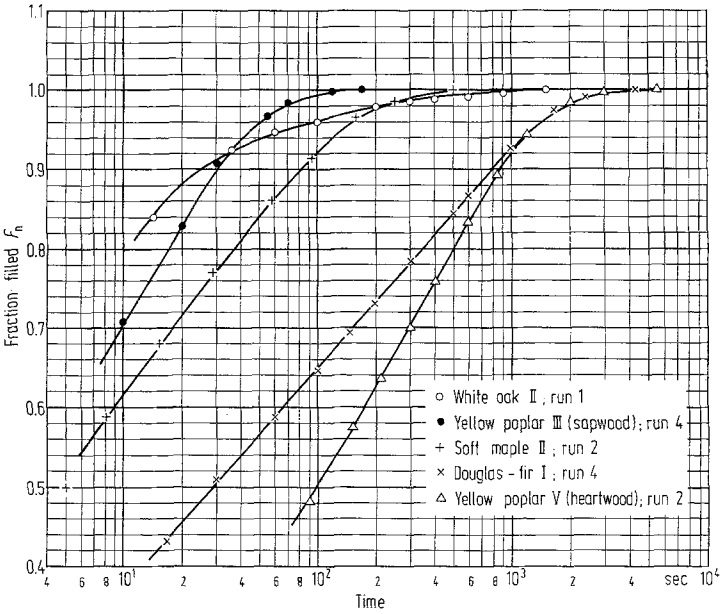

Fig. 12. Transverse permeability of four species. Specimens endcoated; Helium; $T = 40$ °C; $p_{eq} = 331 \ldots 354$ Torr.

Table 2. *Transverse Gas Permeability of Several Species*

	Number of specimes	Transverse gas permeability[a] × 10^{12} $(cm)^2$
Douglas-fir	1	1.48[b]
Yellow poplar (heartwood)	2	0.94—1.34
Yellow poplar (sapwood)	1	40.0
Soft maple	1	14.5
White oak	1	50.0[b]

[a] Helium $T = 40°$ C; $P_{eq} = 340$ Torr.

[b] The Douglas-fir and white oak specimens contained drying defects causing the permeability values to be higher than they would have been for perfect specimens.

It must also be stated that there is no particular reason to assume that any of the reported transverse gas permeabilities is near the average for the species.

Variation of Permeability between Douglas-fir Specimens

The variation in gas permeability between different specimens of the same species may be considerable. No attempt was made to obtain yellow poplar specimens representing a wide range of densities, growth rates or growth sites. However, as a preliminary experiment, seven Douglas-fir specimens were run. These specimens were part of a set of 22 Douglas-fir heartwood specimens which were obtained from the Oregon Forest Products Laboratory. These were end-matched with another set used by the Oregon Forest Products Laboratory in a creosote

impregnation study. The full set of 22 represented a large range of variability and the sub-set of seven included virtually both extremes.

The specimens were rectangular, $45 \times 3.8 \times 3.8$ cm; they were not endcoated. The data obtained are not very accurate because of the limited pressure drop which occurs with the small specimen. The data are plotted in Fig. 13. The eighth specimen (C 1), shown in Fig. 13, does not belong to the Oregon set; it was ob-

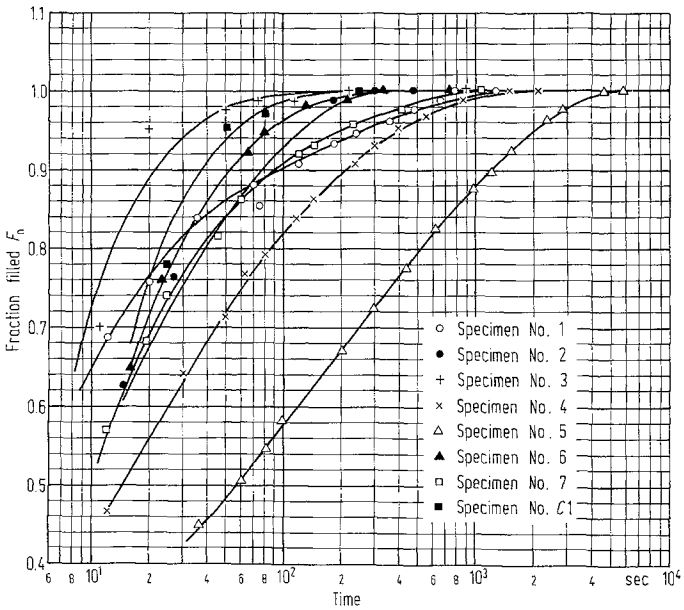

Fig. 13. Variation in gas permeability of Douglas-fir squares. Dimension 45 cm × 3.8 cm × 3.8 cm; Helium; $T = 30$ °C; $p_{eq} = 290$ Torr.

tained by machining the cylindrical specimen identified as Douglas-fir I in Fig. 10 and Table 2 down to the square dimension. Thus, it allows a more meaningful comparison between the two sets of data.

Table 3. *Permeability of Douglas-fir Heartwood Specimens as Determined by Different Methods*

Specimen number	Time required to obtain fraction filled = 0.95 seconds	Creosote permeability number [Miller[1]]	Maximum effective pit pore radius for passage in series through 100 pits [Stamm et al.] μm
3	30	6	0.52
C1	55	—	—
6	80	2.5	0.055
2	120	3.5	0.08
7	200	3.5	0.035
1	260	—	—
4	410	2	0.02
5	2000	1.5	0.025

[1] Arbitrary scale in which 6 indicates almost complete penetration and 1 indicates only a slight penetration.

If one arbitrarily selects a fraction filled of 0.95 as a point of reference, the time needed to reach this level is a practical indicator of permeability. It is roughly proportional to $1/K$. The times give an extreme ratio of 1:67. The correlation of the times with other data obtained by STAMM et al. [1968] on the same specimens and on the matched set by MILLER[1] is quite reasonable, as can be seen in Table 3.

Transverse and Longitudinal Permeability of Yellow Poplar

The results of experiments with and without endcoating (Figs. 10, 11, 12) show that the effect of endcoating is to increase the time to reach a fraction filled of 0.9 by a factor 3.7 to 26. For yellow poplar specimen II (heartwood), the helium permeability experiment was run three ways: with the ends coated, with no coating and with the sides coated. For the latter two experiments, the endcoating was removed by cutting about 0.2 cm off each end. The results of these experiments are shown in Fig. 14. The uncoated specimen cannot be approximated by a simple model, but the side-coated specimen lends itself very readily to model construction. The assumption of 10 zones, each consisting of two slices of $^1/_{20}$ of the specimen

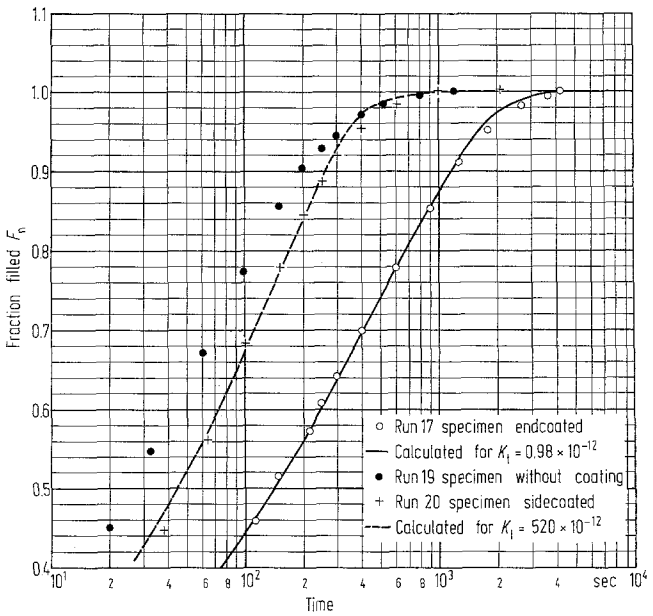

Fig. 14. Comparison of transverse, longitudinal and total permeability. Yellow poplar specimen II heartwood; Helium; $T = 40$ °C; $p_{eq} = 327$ Torr.

length (one on each end), leads to a set of equations similar to the ones for the concentric zone model. In Fig. 14 the solution curves best fitting the experimental data have been drawn. The best fitting longitudinal and transverse gas permeabilities are 520×10^{-12} and 0.98×10^{-12} cm^2, giving a longitudinal/transverse ratio of 530.

[1] Unpublished data from D. J. MILLER, Oregon State University, Corvallis, Oregon.

OSNACH [1961] and SMITH [1963] have given steady-state values for the gas permeability of hardwoods in three axial directions. Using an average of radial and tangential permeability as a transverse value, the longitudinal/transverse ratio for diffuse-porous woods ranges from 2.9×10^3 to 6.05×10^4. Ring-porous woods exhibit somewhat higher ratios with red oak at an extreme level of 3.3×10^5.

The main reason for the difference between the author's value of 530 and the others quoted is likely to be the geometry of the specimens. In a large specimen, as used in the present study, transverse flow may occur to a large extent by longitudinal paths, using the transverse cross-over points which have the lowest resistance.

Some Evidence in Support of the Slip Flow Theory

The occurrence of slip flow depends on whether the mean free path of the gas molecules approaches the capillary radius. The lumen radii of vessels and fibers in yellow poplar are in the order of 40 μm and 7 μm. The communicating pit membrane pores are at least an order of magnitude smaller [BROWN et al. 1949; HAYWOOD 1950]. The mean free path of helium, calculated from viscosity data is 53 μm at 300 Torr, 32 μm at 500 Torr, 23 μm at 700 Torr and 18 μm at 900 Torr. It appears possible that slip flow occurs. However, in a single experimental run the effect cannot be detected, because of the way the experiment is conducted. The mean pressure stays constant during the run. Also, the pressure of the surroundings, which is the pressure at which the gas enters the specimen, varies only a moderate amount during that part of the run where the data are collected. For example, the external pressure for the points plotted in Fig. 8 varied from 460 Torr to 329 Torr.

If different equilibrium pressures are employed in different runs, a comparison of superficial permeabilities found at the different average pressures will permit the calculation of the b constant in Klinkenberg's equation [1941].

$$K = K_\infty \left(1 + \frac{b}{p}\right). \tag{6}$$

Fig. 15 gives fraction filled as a function of time for three levels of equilibrium pressure. The mass flow is proportional to the square of the pressure. When flow is expressed as a fraction of the total number of moles, it is proportional to the pressure. If slip flow did not occur, the apparent permeabilities would be the same for the different levels of equilibrium pressure. Then the curves in Fig. 15 should be separated by a distance equal to the ratio of the pressures. It can be observed that this is not the case.

When the best fitting curves are drawn for each run, the superficial permeability may be calculated for each run. This has been done for the three runs shown in Fig. 15 and for another set of three runs on a different specimen. Since the constant b can only be evaluated from a comparison of two permeability values, the six runs give four independent estimates of b. Table 4 gives the observed values of transverse gas permeability for each of the six runs and the value calculated from Klinkenberg's equation and the best estimate of K_∞. The agreement between the observed and calculated values for the superficial permeability would be much

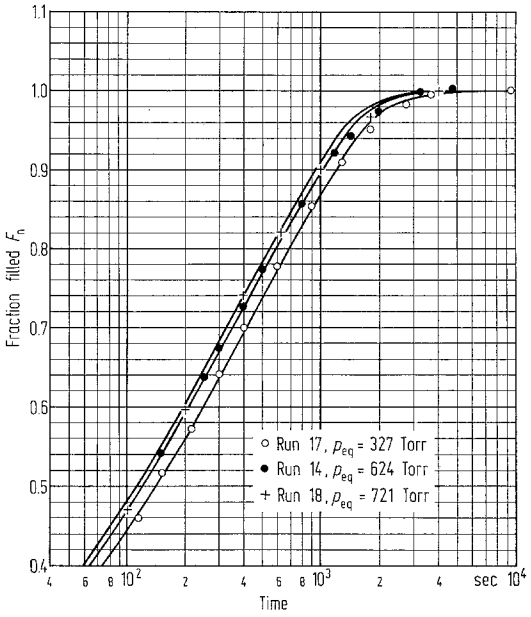

Fig. 15. Permeability of yellow poplar specimen II heartwood, for different levels of equilibrium pressure. Helium; T = 40 °C.

Table 4. *Comparison of Superficial Permeabilities Observed and Calculated with the Aid of Klinkenberg's Equation*

Uellow poplar specimen and run number	Equilibrium pressure Torr	Superficial permeability observed $\times 10^{12}$ cm²	Superficial permeability calculated $\times 10^{12}$ cm²
# II, Run 17	327	0.98	0.95[a]
# II, Run 14	624	0.60	0.61[a]
# II, Run 18	721	0.55	0.56[a]
# V, Run 3	333	1.34	1.47[b]
# V, Run 7	690	0.96	0.90[b]
# V, Run 6	939	0.79	0.77[b]

[a] Calculated for $K_\infty = 0.243 \times 10^{-12}$ cm² and b = 949 Torr.
[b] Calculated for $K_\infty = 0.381 \times 10^{-12}$ cm² and b = 949 Torr.

better if one were to assume different values of b for each of the two yellow poplar specimens. It was felt that there was not sufficient reason to do this, and the value of 949 Torr for b was the average of four calculations, two for each specimen. The agreement is good enough to be interpreted as evidence supporting the essential validity of Klinkenberg's equation.

Specific Gravity of Wood Substance

While the purpose of the experiments was to study permeability phenomena, a by-product of the work is that each helium run yields a determination of the specific gravity of wood substance. At a temperature of 40 ° C, there is no ab-

sorption of helium. This has been demonstrated with charcoal experiments by HOWARD and HULETT [1924]. Therefore, the volume occupied by the helium at equilibrium can be determined accurately from the equilibrium pressure by application of the ideal gas law[1].

$$V_{eq} = \frac{P_i V_i}{P_{eq}} \tag{5}$$

where the subscript i indicates the initial and the subscript eq the equilibrium condition. When the volume V_{eq} is subtracted from the total volume of the system, the volume of the wood substance is found.

The most consistent results were obtained when the system had been recently calibrated. Seven determinations on yellow poplar heartwood gave an average specific gravity of wood substance of 1.465, and four determinations on soft maple sapwood gave an average specific gravity of wood substance of 1.473. The individual determinations are given in Table 5. The values obtained are in excellent agreement with those found by WILFONG [1966].

Table 6. *Specific Gravity of Wood Substance for Selected Runs*

Species	Specific gravity of wood substance		
	Individual	Average	Standard Deviation
Yellow poplar heartwood	1.463		
Yellow poplar heartwood	1.460		
Yellow poplar heartwood	1.464		
Yellow poplar heartwood	1.473	1.465	
Yellow poplar heartwood	1.472		
Yellow poplar heartwood	1.457		
Yellow poplar heartwood	1.463		0.006
Soft maple sapwood	1.463		
Soft maple sapwood	1.481	1.473	
Soft maple sapwood	1.470		
Soft maple sapwood	1.477		

Conclusions

The experimental results confirm that Darcy's flow equation holds approximately for the flow of helium through wood, when the pressure in the system remains close to a level p for which the superficial permeability is calculated. There is evidence that some species have a nearly uniform transverse gas permeability. Other species exhibit a multi-level transverse permeability. For the purpose of predicting gas flow in these species, it is sufficient to assume only two levels of transverse gas permeability.

[1] The assumption of ideality gives an error of approximately 0.15 percent in the volume thus calculated. However, the volume of the small cylinder was calculated from the measured volume of the large cylinder by making several empty runs and applying the ideal gas law to the average pressure ratio. This way, the errors substantially cancel each other.

The unsteady-state technique employed in these experiments is particularly useful to measure permeability in a practical sense. The results of such measurements are applicable to commercial processes.

In addition to the major conclusions given above, it appears that the unsteady state method is quite useful as a research method in the following areas.

1. Variation of gas permeability within species.
2. Variation of gas permeability between species.
3. Effect of drying technique on gas permeability of dry wood.
4. Slip flow effect.
5. Specific gravity of wood substance.
6. Permeability and absorption/condensation phenomena of non-ideal gases in wood.

A major drawback of the technique is that with the instrumentation described in this paper, it becomes difficult to make accurate observations on highly permeable wood species. Automatic recording equipment would be preferred.

References

BAILEY, I. W.: The preservative treatment of wood — The validity of certain theories concerning the penetration of gases and preservatives into seasoned wood. Forestry Quarterly **11** (1913) 5—11.

BROWN, H. P., A. J. PANSHIN and C. C. FORSAITH: Textbook of Wood Technology, Vol. I. New York 1949: McGraw-Hill Book Company Inc.

BUCKMAN, S. J., H. SCHMITZ and R. A. GORTNER: A study of certain factors influencing the movement of liquids in wood. J. Phys. Chem. **39** (1935) 103—120.

COMSTOCK, G. L.: Longitudinal permeability of green eastern hemlock. For. Prod. J. **15** (1965) 441—449.

— Longitudinal permeability of wood to gases and nonswelling liquids. For. Prod. J. **17** (1967) 41—47.

HAYWOOD, G.: Effect of variations in size and shape of fibers on papermaking properties. Tappi **33** (1950) 370—383.

HOWARD, H. C., and G. A. HULETT. A study of the density of carbon. J. of Phys. Chem. **28** (1924) 1082—1095.

KLINKENBERG, L. J.: The permeability of porous media to liquids and gases. Drilling and Production Practice, pp. 200—213. The American Petroleum Institute 1941.

OSNACH, N. A.: O pronitsaemosti drevesini. Derevoobrabaty-valuschaia promyshlennost **10** (1961) 11—13.

PFALZNER, P. M.: On the flow of gases and water vapor through wood. Canad. J. Res. **28 A** (1950) 389—410.

RESCH, H.: Unsteady-state flow of compressible fluids through wood. For. Prod. J. **17** (1967) 48—54.

— and B. A. ECKLUND: Permeability of wood—Exemplified by measurements on redwood. For. Prod. J. **14** (1964) 199—206.

SEBASTIAN, L. P., W. A. CÔTÉ and C. SKAAR: Relationship of gas permeability to ultrastructure of white spruce wood. For. Prod. J. **15** (1965) 394—404.

SMITH, D. N.: The permeability of wood to liquids and gases. Food and Agriculture Organisation of the United Nations—Fifth Conference on Wood Technology, 1963.

STAMM, A. J.: The capillary structure of softwoods. J. Agric. Res. **38** (1929) 23—67.

— S. W. CLARY and W. J. ELLIOTT: Effective radii of lumen and pit pores in softwoods. Wood Science **1** (1968) 93—101.

WILFONG, J. G.: Specific gravity of wood substance. For. Prod. J. **16** (1966) 55—61.

(Received December 27, 1968)

Dr. ANCO L. PRAK
Associate Professor in Industrial Engineering
North Carolina State University at Raleigh
Raleigh, N.C. 27607, U.S.A.